BMC Plant Biology

RESEARCH Open Access

Unveiling the impact of nitrogen deficiency on alkaloid synthesis in konjac corms (*Amorphophallus muelleri* Blume)

Ying Qi[1], Penghua Gao[1], Shaowu Yang[1], Lifang Li[1], Yanguo Ke[1], Yongteng Zhao[1], Feiyan Huang[1*†] and Lei Yu[1*†]

Abstract

Background Konjac corms are known for their alkaloid content, which possesses pharmacological properties. In the primary cultivation areas of konjac, nitrogen deficiency is a common problem that significantly influences alkaloid synthesis. The impact of nitrogen deficiency on the alkaloids in konjac corms remains unclear, further complicated by the transition from mother to daughter corms during their growth cycle.

Results This study examined 21 alkaloids, including eight indole alkaloids, five isoquinoline alkaloids, and eight other types of alkaloids, along with the associated gene expressions throughout the development of *Amorphophallus muelleri* Blume under varying nitrogen levels. Nitrogen deficiency significantly reduced corm diameter and fresh weight and delayed the transformation process. Under low nitrogen conditions, the content of indole alkaloids and the expression of genes involved in their biosynthesis, such as tryptophan synthase (TRP) and tryptophan decarboxylase (TDC), exhibited a substantial increase in daughter corms, with fold changes of 61.99 and 19.31, respectively. Conversely, in the mother corm, *TDC* expression was markedly reduced, showing only 0.04 times the expression level observed under 10 N treatment. The patterns of isoquinoline alkaloid accumulation in corms subjected to nitrogen deficiency were notably distinct from those observed for indole alkaloids. The accumulation of isoquinoline alkaloids was significantly higher in mother corms, with expression levels of aspartate aminotransferase (GOT), chorismate mutase (CM), tyrosine aminotransferase (TAT), and pyruvate decarboxylase (PD) being 4.30, 2.89, 921.18, and 191.40 times greater, respectively. Conversely, in daughter corms, the expression levels of *GOT* and *CM* in the 0 N treatment were markedly lower (0.01 and 0.83, respectively) compared to the 10 N treatment.

Conclusions The study suggests that under nitrogen deficiency, daughter corms preferentially convert chorismate into tryptophan to synthesize indole alkaloids, while mother corms convert it into tyrosine, boosting the production of isoquinoline alkaloids. This research provides valuable insights into the mechanisms of alkaloid biosynthesis in *A. muelleri* and can aid in developing nitrogen fertilization strategies and in the extraction and utilization of alkaloids.

†Feiyan Huang and Lei Yu contributed equally to this work.

*Correspondence:
Feiyan Huang
125593879@qq.com
Lei Yu
yulei0425@163.com

Full list of author information is available at the end of the article

Keywords Nitrogen deficiency, Precursor amino acid, Alkaloid, Nitrogen fertilization strategie, *Amorphophallus Muelleri* Blume

Introduction

Konjac is a name for certain species within the genus *Amorphophallus*, belonging to the family Araceae [1]. Valued as an important cash crop, konjac corms are consumed as a vegetable and utilized in traditional medicine for their detoxifying and anti-inflammatory properties across China and Southeast Asia [2–4]. These corms contain various alkaloids that are crucial for their medicinal effects [5]. However, due to the alkaloids, direct consumption or skin contact can cause adverse reactions such as redness, swelling, and irritation of the throat and skin [6, 7]. It is thus essential to precisely control the alkaloid content when using konjac for different applications. Konjac plants renew their corms annually, with a corm typically lasting less than two years. This renewal results in no more than two age groups of corms coexisting within a plant. Nonetheless, the variations and patterns of alkaloid accumulation in corms of different ages remain unclear.

Alkaloids are a varied group of nitrogen-containing natural products with distinct biosynthetic pathways [8–10]. Originating from primary metabolites such as amino acids [11], alkaloids are classified based on their precursor amino acids [12]. Among the most prevalent are indole and isoquinoline alkaloids, known for their anti-inflammatory [13], antitumor [14], and antimicrobial properties [15]. Furthermore, the availability of nitrogen affects alkaloid biosynthesis [16–18]. As a vital element of the photosynthetic machinery, nitrogen impacts the production of secondary metabolites such as alkaloids by influencing photosynthesis and primary metabolism [19].

Alkaloids, nitrogen-containing secondary metabolites, are typically produced by plants for protection against herbivores, pathogenic bacteria, or to handle abiotic stresses [20]. Nitrogen deficiency significantly impacts alkaloid synthesis; for example, *Lupinus micranthus* showed a 9–17% reduction in total alkaloid content under nitrogen deficiency, although the content may increase once nitrogen supply is restored [21]. However, nitrogen deficiency can also enhance the accumulation of berberine in the roots of *Coptis chinensis* [22] and increase the total alkaloid and goitrin content in *Isatis tinctoria* [23], indicating inconsistent effects of nitrogen on alkaloid accumulation in plants.

The primary soil types in the konjac planting area are acrisols and alisols [24], which tend to leach nutrients due to heavy rainfall and high temperatures, resulting in relatively infertile soils, particularly deficient in nitrogen [3]. The impact of nitrogen deficiency on alkaloids in konjac corms remains unclear, especially considering the transformation from mother to daughter corms during the growth cycle. Nitrogen plays a crucial role in plant metabolism; its deficiency leads to slower growth, reduced yields, and enhanced stress tolerance, which may compromise growth [25]. This balance between growth and defense is crucial for plant survival and has significant implications for agriculture and natural ecosystems [26, 27].

This study explores the dynamic changes in corm alkaloids throughout the growth cycle of *Amorphophallus muelleri* Blume, comparing alkaloid composition and gene expression in corms treated with varying nitrogen levels. This research marks the first examination of alkaloid accumulation during konjac corm turnover under nitrogen deficiency. Understanding this process is essential for developing more effective nitrogen fertilization strategies and improving alkaloid extraction methods in *A. muelleri*.

Materials and methods

Plant materials, growth conditions, and treatment

The corms of *Amorphophallus muelleri* Blume were obtained from Konjac Genetic Resource Garden of Kunming University, Yunnan Province (24.98°N, 102.79°E; altitude: 1934 m). Uniformly sized and weighted (approximately 100 g) corms of *A. muelleri* were selected and planted in 10 L plastic pots filled with around 8 L of perlite as the growing medium, primarily consisting of silica and little to no nitrogen. The experiment was conducted in a greenhouse at the Yunnan Urban Agricultural Engineering and Technological Research Center of Kunming University from May to November 2022. The greenhouse conditions were maintained at temperatures in the range of 25–35 °C, less than 50% shade, and 60–80% relative humidity. Watering was performed as needed, and liquid fertilizer was applied at 500 mL per pot every three days post-sprouting. The basic liquid fertilizer composition included various minerals and trace elements (2 mM $MgSO_4$, 2 mM $CaCl_2$, 3 mM KCl, 1 mM NaH_2PO_4, 13 mM $FeSO_4$-Na_2EDTA, 0.1 mM $MnSO_4$, 1 μM $CuSO_4$, 0.1 mM H_3BO_3, 0.05 mM $ZnSO_4$, and 5 μM KI). The sole nitrogen source was NH_4NO_3 at concentrations of 0 mM (the substrate contained no nitrogen and was not fertilized with N; 0 N), 5 mM (5 N), and 10 mM (reflecting local average nitrogen application rates).

Sampling time, corm biomass, and the measurement of nitrogen content

Figure 1A illustrates dormant corms (D) stored at 20 °C for 2 weeks without sprouting [28]. Corms with buds

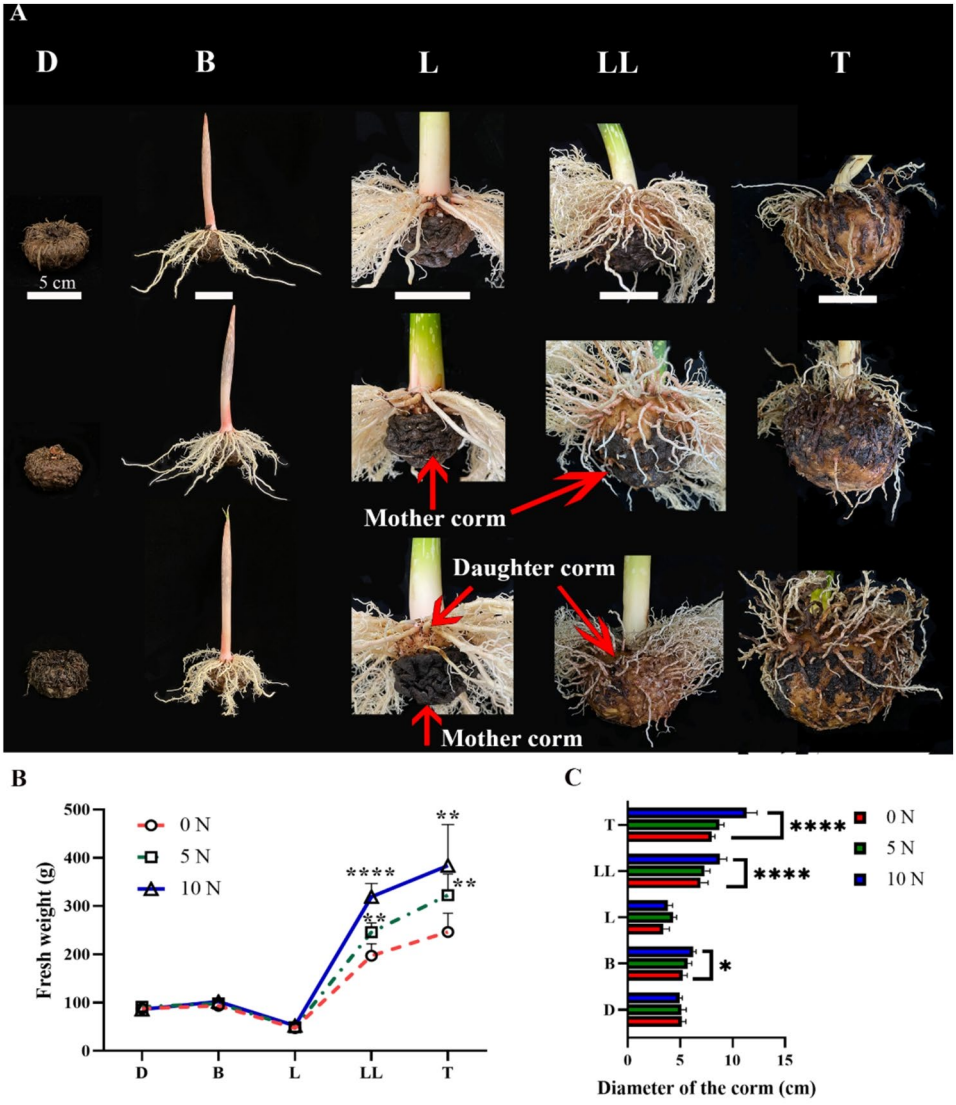

Fig. 1 Effect of nitrogen deficiency on corms of *A. muelleri* during the growth cycle. Diagram illustrating corm growth in *A. muelleri* (**A**). Changes in the fresh weight (**B**) and diameter (**C**) of corms during the growth cycle are shown. Abbreviations: D: dormant corms; B: bud sprouting stage; L: first leaf maturation stage; LL: second leaf maturation stage; T: lodging period. Each data point represents the mean ± SE ($n \geq 6$). The different letters above the bars indicate significant differences between developmental periods ($P < 0.05$; based on one-way ANOVA followed by a post hoc Tukey's test)

germinating between 5 and 8 cm served as materials for the bud sprouting stage (B). Upon full expansion of the first leaf, the mother corm diminishes, and the daughter corm starts growing, marking the first leaf maturation stage (L), designated as L and L′. At full expansion of the second leaf, mother and daughter corms mark the second leaf maturation stage (LL), noted as LL and LL′. During the lodging period (T), when the second leaves wither, corm measurements including fresh weight and diameter (the maximum distance from one rim to another through the center) were taken, with at least six corms measured per period.

Nitrogen content was assessed using a Flash 2000 Elemental Analyzer (Thermo Fisher Scientific, Waltham, MA, USA). The process involves burning samples at high temperatures to generate N_2 for mass spectrometry, with nitrogen content (N%) derived by comparing sample peak areas to two or three standards (Atm-N_2).

Metabolomic analysis

For metabolite profiling during the growth cycle, corm samples were collected approximately 5 mm below the buds. Metabolites were extracted by pulverizing 50 mg of sample in liquid nitrogen and adding 400 µL of a 4:1 methanol: water solution containing 0.02 mg/mL of L-2-chlorophenylalanine. The mixture was sonicated for 30 min at 5 °C and 40 kHz, then stood at −20 °C for 30 min, followed by centrifugation at 4 °C and 13,000 g

for 15 min. The supernatant was then transferred to an injection vial for analysis. To ensure quality control, we prepared samples by mixing equal volumes of metabolites from all samples and inserted a quality control sample every 5–10 samples during analysis. A principal component analysis (PCA) of the normalized data was conducted using metaX software [29].

The untargeted metabolomics assay was performed using a Thermo UHPLC-Q Exactive HF-X system, equipped with an Acquity HSS T3 column (100 mm × 2.1 mm i.d., 1.8 μm; Waters, USA) at Majorbio BioPharm Technology in Shanghai, China. The mobile phases included 0.1% formic acid in a water/acetonitrile mixture (95:5, v/v, solvent A) and 0.1% formic acid in an acetonitrile/isopropanol/water mixture (47.5:47.5:5, v/v/v, solvent B). The flow rate was set at 0.40 mL/min and the column temperature maintained at 40 °C.

For sample mass spectrometry signal acquisition, both positive and negative ion scanning modes were utilized. The optimal settings were as follows: source temperature at 425 °C; mass scanning range (m/z) from 70 to 1050; ion-spray voltage set to 3500 V for both modes; sheath gas at 40 psi; auxiliary heated gas at 10 psi; cyclic collision energy varying from 20 to 60 V; full MS resolution at 60,000; and MS/MS resolution at 7,500.

RNA-seq analysis

Total RNA was extracted from corms positioned approximately 5 mm below the buds using TRIzol® Reagent (Invitrogen, CA, USA), following the manufacturer's protocol. RNA quality was assessed using a 5300 Bioanalyzer (Agilent, CA, USA) and quantified using a NanoDrop-2000 (Thermo Fisher Scientific). Only high-quality RNA (OD260/280 ratio between 1.8 and 2.2, OD260/230 ratio above 2.0, RIN above 6.5, 28 S:18 S ratio above 1.0, and a minimum quantity of 1 μg) was selected for sequencing library construction. The quality and concentration details of the extracted RNA are provided in Table S1.

RNA purification, reverse transcription, library construction, and sequencing for all treatments (0 N, 5 N, and 10 N) were conducted at Shanghai Majorbio Biopharm Biotechnology (Shanghai, China), following the guidelines from Illumina (CA, USA). The cDNA libraries were prepared using a NEBNext® UltraTM RNA Library Prep Kit for Illumina® (NEB, USA) in accordance with the supplied protocol. Sequencing was carried out on an Illumina Hiseq 4000 platform. After measurement with Qubit 4.0, the paired-end RNA-seq libraries were sequenced on a NovaSeq 6000 sequencer, producing reads of 2×150 bp. The initial quality check of these reads was managed using fastp with standard settings. Subsequently, clean data from all treatments underwent de novo assembly using Trinity [30]. To enhance the assembly quality, all sequences were further refined using CD-Hit and transrate.

Metabolic pathway analysis utilized the Kyoto Encyclopedia of Genes and Genomes (KEGG). We conducted differential expression analysis and functional enrichment to pinpoint differentially expressed genes (DEGs) between the treatments. Gene expression levels were determined using the transcripts per million reads method. RNA-seq by expectation maximization was employed to quantify gene abundance [31]. Differential expression was analyzed using DESeq2 [32], with DEGs identified based on $|\log2FC| \geq 1$ and $FDR \leq 0.05$, signifying significant differential expression. Additionally, a KEGG functional enrichment analysis determined which DEGs were significantly enriched in metabolic pathways, with significance set at a Bonferroni-corrected $P \leq 0.05$ compared to the entire transcriptome. KEGG pathway analysis was performed using KOBAS [33].

Gene co-expression network construction

To evaluate the relationship between alkaloid content and gene expression levels in konjac corms, we conducted a gene co-expression network analysis utilizing the Weighted Gene Co-expression Network Analysis (WGCNA) package in R [34]. We identified 17,772 differentially expressed transcripts from the 0 N versus 10 N treatments across all three developmental stages of new corms using the DESeq2 package in R. Transcripts were considered differentially expressed if the adjusted p-value < 0.05 and the fold change > 2.

The soft threshold was calculated utilizing the pickSoftThreshold package in R. Subsequently, a scale-free network was constructed based on the power value at which the fitted curve initially approached 0.8, identified as a power value of 9. The eigenvector values for each module were computed and subjected to clustering, with modules exhibiting a similarity greater than 75% being merged. The content of 21 alkaloids were employed as traits to calculate the correlation coefficients between alkaloid levels and gene expression abundance within each module under varying nitrogen treatments. The TOM matrix was computed utilizing the TOMsimilarityFromExpr function in R, while the connectivity of individual genes within the module was determined using the softConnectivity function. The gene co-expression network was visualized by Cytoscape version 3.10.0 [35].

Real-time quantitative PCR analysis (RT-qPCR)

RT-qPCR was used to examine gene expression in the indole and isoquinoline alkaloid synthesis pathways in corm samples of *A. muelleri* previously analyzed by RNA-seq. RNA extraction utilized TRIzol® Reagent, and first-strand cDNA synthesis followed the TUREscript 1st Stand cDNA Synthesis Kit's instructions (Aidlab, Beijing,

China). Primers were designed using Beacon Designer 7.9 (refer to Table S2). The RT–qPCR was conducted on a qTOWER 2.0/2.2 Quantitative Real-Time PCR Thermal Cycler (Langewiesen, Germany), employing the ΔCt method to calculate gene expression levels. Transcript levels for eight housekeeping genes (*Actin*, *GAPDH*, *18SrRNA*, *EF-1β*, *QCR*, *β-Tubulin*, *CYP*, and *SAMDC*) were measured, and the geNorm algorithm identified *Actin* as the most stable reference gene [36]. Each analysis was performed at least three times with biological replicates.

Statistical analysis

To assess growth traits and metabolite contents in the corms over different periods, one-way ANOVA and a subsequent Tukey's post hoc test were conducted using SPSS version 16.0 (IBM, USA). A $p<0.05$ was deemed significant. For two-group comparisons, Student's t-test was used, with a significance threshold of $p<0.05$. Each treatment was replicated at least three times biologically. Heat maps were created using TBtools [37], with data $\log_2$ transformed and hierarchical clustering performed through Pearson's correlation distance/complete linkage. GraphPad version 9.0 (GraphPad Software, MA, USA) was used for other bar chart visualizations.

Results

Effect of nitrogen deficiency on the growth of corms during the growth cycle

Nitrogen deficiency treatments (0 N and 5 N) negatively impacted the growth of daughter corms (Fig. 1A), resulting in lighter weights (Fig. 1B) and smaller diameters (Fig. 1C) compared to the 10 N treatment. For instance, at the lodging stage (T), corms treated with 10 N had a diameter of 11.33 cm, which was 1.29 times that of those treated with 5 N (8.73 cm) and 1.42 times that of those treated with 0 N (8 cm).

Furthermore, nitrogen deficiency delayed the transition from mother to daughter corms, prolonging the growth cycle and reducing yield. At the first leaf maturation stage (L), the fresh weight of daughter corms in the 0 N treatment was only 12.53 g, representing 36% of the fresh weight of mother corms (34.62 g). In contrast, in the 10 N treatment, the fresh weight of daughter corms was 26.94 g, which was 107% of the fresh weight of mother corms (25.27 g). By the second leaf maturation stage, mother corms in the 10 N treatment had almost completely been absorbed, resulting in a new corm weight of 384.01 g, 4.46 times that of the dormant stage. Conversely, treatments 5 N and 0 N retained some mother corms, with the fresh weight of daughter corms in the 0 N treatment at 246.65 g, which was 76% of that in the 5 N treatment and 64% of that in the 10 N treatment (Table S3).

Metabolomic profiles in response to nitrogen deficiency

During the growth cycle, the nitrogen content in mother corms exhibited a decline, whereas the nitrogen content in daughter corms initially decreased and subsequently increased (Fig. 2A). The effect of nitrogen deficiency on the nitrogen content in mother and daughter corms varied (Fig. 2A; Table S4). Under the 0 N and 5 N treatments, the nitrogen content in daughter corms at the L' stage was either reduced or remained approximately constant compared to the T stage. However, in the 10 N treatment, nitrogen content in daughter corms increased throughout development; it was 1.52 times higher at the T stage than at the L' stage, and 2.68 times higher than in 0 N-treated corms at the same stage.

In mother corms, we found that the nitrogen application mitigated the declining trend in nitrogen content, for instance, at the end of development (LL), nitrogen content in the 10 N treatment was 0.94%, only 39% of the content at the dormancy stage (D), while in the 0 N treatment, it was 1.39%, or 57% of the nitrogen content at the D stage.

To analyze metabolomic changes in *A. muelleri* due to nitrogen deficiency, we identified 2250 metabolites in corms across 0 N, 5 N, and 10 N treatments using untargeted metabolomics (Table S5). Principal component analysis (PCA) demonstrated the impact of different nitrogen concentrations on corm metabolites. Metabolite profiles in the 0 N and 10 N treatments were distinctly separated by PC1, explaining 38.70% of the variance, and PC2, explaining 25.50% (Fig. 2B). Notably, metabolite differences were clear between mother and daughter corms; in daughter corms, 597 metabolites were downregulated and 358 upregulated from 0 N to 10 N, whereas in mother corms, 388 were downregulated and 274 upregulated (Fig. 2C). To further explore these changes, we conducted KEGG enrichment analysis (Fig. 2D, E). In mother corms, differential metabolites were primarily enriched in pathways like "plant hormone signal transduction," "tricarboxylic acid cycle," and "isoquinoline alkaloid biosynthesis." In daughter corms, significant enrichment was noted in "phenylpropanoid biosynthesis," "tryptophan metabolism," and "indole alkaloid biosynthesis." Both "isoquinoline alkaloid biosynthesis" in mother corms and "indole alkaloid biosynthesis" in daughter corms showed significant enrichment, highlighting their role in alkaloid synthesis from 0 N to 10 N treatments.

Comparison of alkaloid content under nitrogen deficiency

To examine the impact of nitrogen deficiency on alkaloid content in *A. muelleri* corms, we analyzed 21 alkaloids under various nitrogen concentrations (Fig. 3; Table S6). These included eight indole alkaloids, five isoquinoline alkaloids, and eight other alkaloid types. Significant differences in alkaloid accumulation were observed

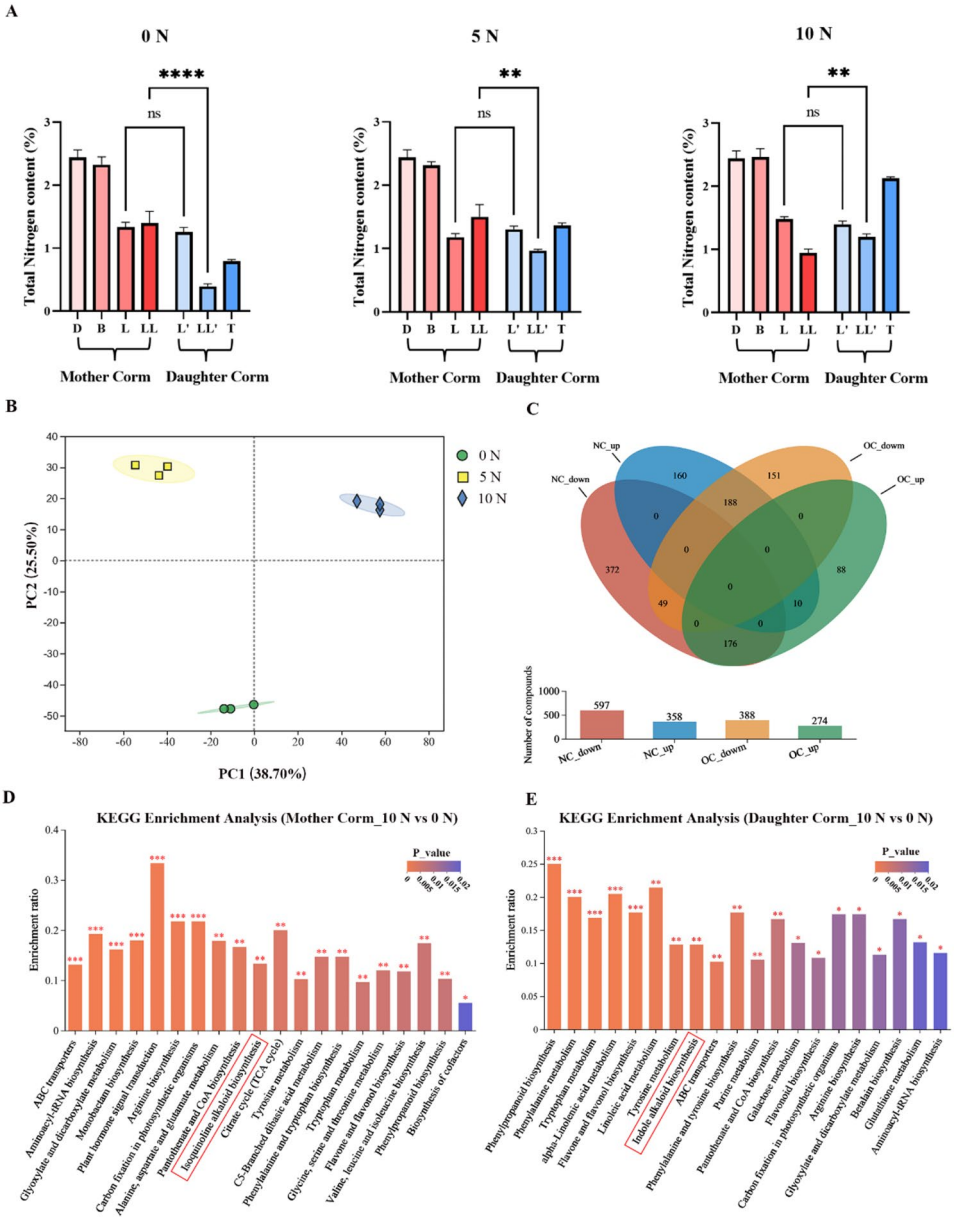

Fig. 2 Analysis of nitrogen content and differential metabolites in corms subjected to different nitrogen concentrations. Effect of nitrogen deficiency on the total nitrogen content during the development of corms (**A**). Red bars represent mother corms and blue bars represent daughter corms, with deeper colors indicating a later developmental period. Principal component analysis of corm samples under nitrogen deficiency (**B**). Venn diagram of differential metabolites in corms (**C**). Kyoto Encyclopedia of Genes and Genomes enrichment analysis of differential metabolites compared between the 0 N and 10 N treatments in mother corms (**D**) and daughter corms (**E**). Asterisks indicate statistical significance based on one-way ANOVA with Tukey's test (*$p < 0.05$; **$p < 0.01$; ***$p < 0.001$; ****$p < 0.0001$)

between daughter and mother corms under different nitrogen treatments (Fig. 3). Indole alkaloids were more prevalent in 0 N-treated mother corms and in 5 N- and 10 N-treated daughter corms. Conversely, isoquinoline alkaloids were more common in 5 N- and 10 N-treated mother corms and in 0 N-treated daughter corms.

We analyzed the variation in the content of indole alkaloids (Fig. 4) and isoquinoline alkaloids (Fig. 5) during the development of konjac corms under different nitrogen treatments (0 N, 5 N, and 10 N). The indole alkaloid content decreased significantly in the mother corms but increased in the daughter corms under the 0 N treatment (Fig. 4A–D). In the 0 N treatment, the halmalol content in mother corms during the first (L) and second (LL) leaf maturation stages was only 40.35% and 36.50%, respectively, of that observed in the 10 N treatment for the same stages. Conversely, the halmalol content in daughter corms during the L' and LL' stages was 2.21 and 2.79

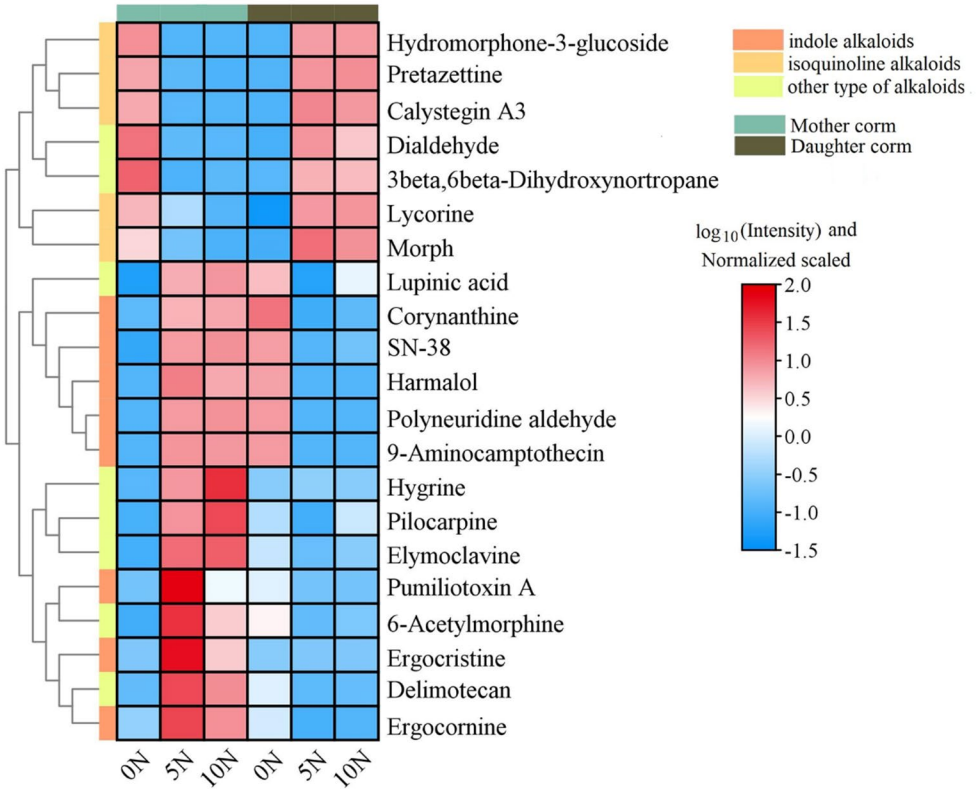

Fig. 3 Effect of nitrogen deficiency on the content of 21 alkaloids in daughter and mother corms of *A. muelleri*

times higher, respectively, compared to the 10 N treatment (Fig. 4A). Similar trends were noted in other indole alkaloids, including ergocornine (Fig. 4B), pumiliotoxin A (Fig. 4C), and corynanthine (Fig. 4D), which also exhibited significant changes.

The accumulation of isoquinoline alkaloids in corms under nitrogen deficiency showed distinct patterns compared to indole alkaloids. In mother corms, isoquinoline alkaloid content, such as hydromorphone-3-glucoside (Fig. 5A), during the L and LL phases was 1.12 and 1.81 times higher in the 0 N treatment than in the 10 N treatment. However, in daughter corms, the content of hydromorphone-3-glucoside during the L' and LL' stages was only 53% and 37%, respectively, of that in the 10 N treatment. Other isoquinoline alkaloids, such as calystegin A3 (Fig. 5B) and morph (Fig. 5C), also followed similar patterns in response to nitrogen deficiency.

KEGG enrichment analysis of DEGs under nitrogen deficiency

To understand the biological functions of genes differentially expressed between the 0 N and 10 N treatments, we conducted KEGG enrichment analysis (Fig. 6). The analysis revealed that genes upregulated in both mother and daughter corms were associated with pathways such as plant hormone signal transduction and plant-pathogen interactions. Downregulated genes were primarily involved in flavonoid biosynthesis.

Notably, the expression trends for genes in mother and daughter corms were opposite. For example, genes related to starch and sucrose metabolism were upregulated in mother corms but downregulated in daughter corms under the 0 N treatment. Similarly, isoquinoline alkaloid biosynthesis genes were upregulated in mother corms, while downregulated in daughter corms, and tropane, piperidine, and pyridine alkaloid biosynthesis genes were also downregulated. Additionally, the nitrogen metabolism pathway was significantly downregulated in daughter corms under the 0 N treatment.

Weighted gene coexpression network analysis

To explore the gene regulatory network involved in alkaloid biosynthesis in *A. muelleri* corms, an analysis of 17,772 differentially expressed transcripts was conducted. This revealed four coexpression modules (blue, brown, gray, and turquoise) identified in a dendrogram. These modules represent clusters of genes that show high correlation and coexpression (Fig. 7A). The turquoise module, containing 90.62% of the transcripts, showed a positive correlation with isoquinoline alkaloids and a negative correlation with indole alkaloids (Fig. 7B). The network analysis pinpointed 20 hub genes significantly

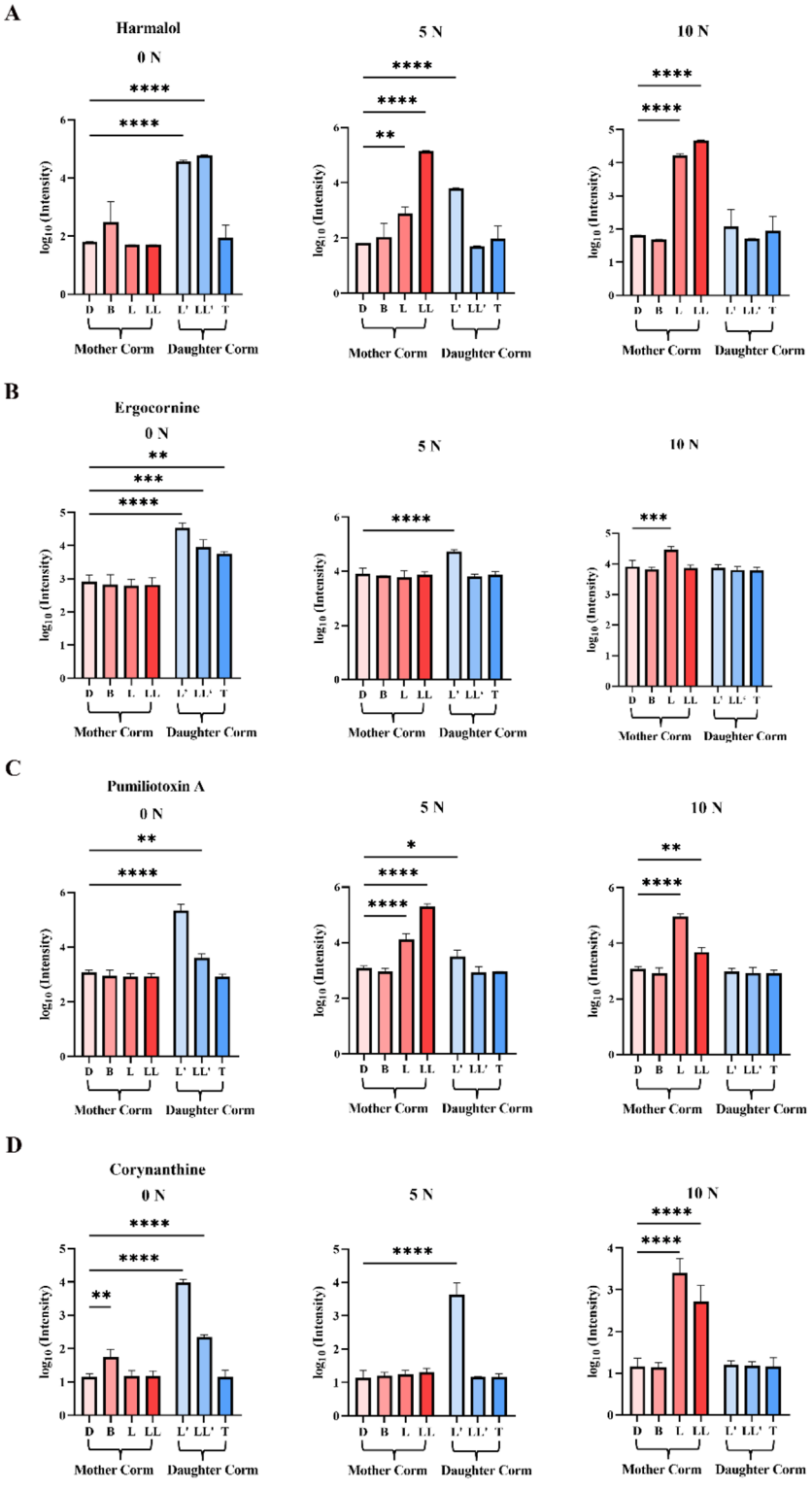

Fig. 4 Trends in the accumulation of four indole alkaloids during the development of corms of *A. muelleri* under nitrogen deficiency. **A**, **B**, **C**, and **D** represent the content of harmalol, ergocornine, pumiliotoxin **A**, and corynanthine, respectively. Red bars represent mother corms and blue bars represent daughter corms, with deeper colors indicating a later developmental period. Asterisks indicate statistical significance based on one-way ANOVA with Tukey's test (ns: not significant; *$p < 0.05$; **$p < 0.01$; ***$p < 0.001$; ****$p < 0.0001$)

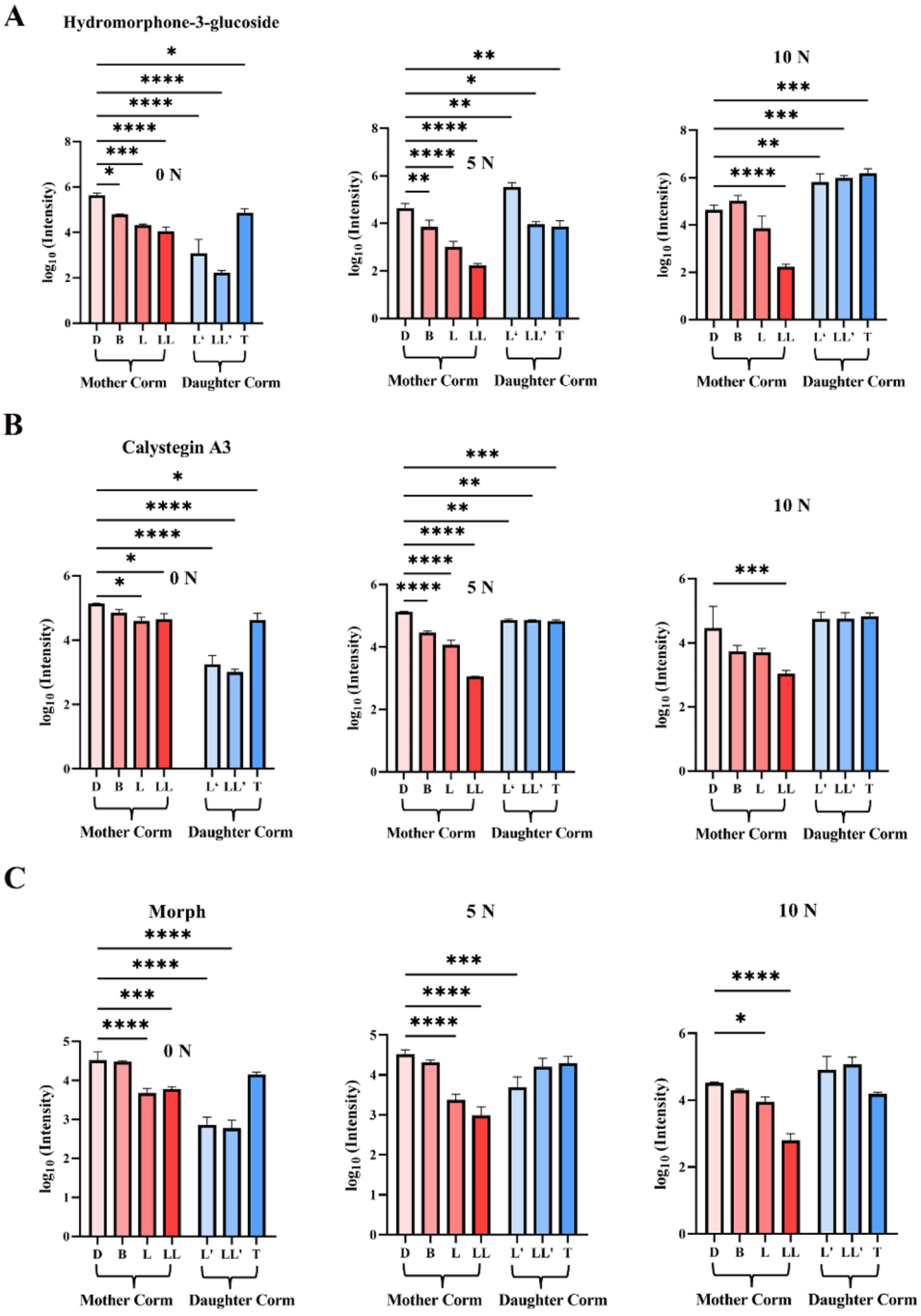

Fig. 5 Trends in the accumulation of three isoquinoline alkaloids during the development of corms of *A. muelleri* under nitrogen deficiency. **A**, **B**, and **C** represent the content of hydromorphone-3-glucoside, calystegin A3 ,and morph, respectively. Red bars represent mother corms and blue bars represent daughter corms, with deeper colors indicating a later developmental period. Asterisks indicate statistical significance based on one-way ANOVA with Tukey's test (*$p < 0.05$; **$p < 0.01$; ***$p < 0.001$; ****$p < 0.0001$)

coexpressed with others, primarily impacting the indole alkaloid biosynthesis pathway. Key genes identified included *TRP* (TRINITY_DN29567_c0_g1) for tryptophan synthase beta chain 2, and a gene for tryptophan dehydrogenase, both crucial for indole alkaloid production. Detailed analysis under nitrogen deficiency revealed 26 genes significantly impacting indole alkaloid synthesis, with 8 downregulated and 18 upregulated (Fig. 7C). Additionally, six genes associated with isoquinoline alkaloid synthesis were all downregulated.

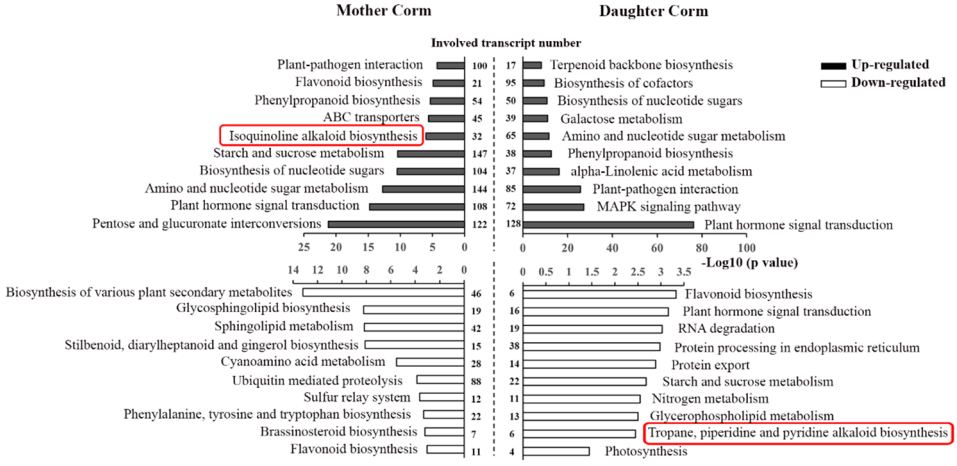

Fig. 6 Kyoto Encyclopedia of Genes and Genomes enrichment analysis of differentially expressed genes in corms of *A. muelleri* compared between the 0 N and 10 N treatments. The left side shows the 10 most enriched pathways in mother corms, and the right side shows the 10 most enriched pathways in daughter corms. Black bars represent upregulation, and white bars represent downregulation. Numbers in the middle are the numbers of transcripts involved in the pathway

Metabolites and genes involved in the indole and isoquinoline alkaloid biosynthesis pathways

Figure 8 highlights notable differences in the biosynthesis of indole and isoquinoline alkaloids between daughter and mother corms under nitrogen deficiency. In mother corms, tryptophan synthase (TRP) expression remained similar across 0 N and 10 N treatments, while in daughter corms, it was significantly higher (61.99 times) in 0 N compared to 10 N. The expression of tryptophan decarboxylase (TDC) and strictosidine synthase (STR1) in mother corms was substantially lower in the 0 N treatment compared to the 10 N treatment, at 0.04 and 0.14 times, respectively. Conversely, in daughter corms, these expressions were 19.31 and 3.21 times higher in the 0 N treatment. Alkaloid content changes showed that in the 0 N treatment, corynanthine and ergocristine levels in mother corms were only 34.82% and 37.04% of those in the 10 N treatment, whereas in daughter corms, levels were 3.32 and 1.95 times higher, respectively, than in the 10 N treatment. These expression profiles are detailed further in Table S7.

Trends in isoquinoline alkaloids in corms under nitrogen deficiency differ significantly from those in indole alkaloids. This study revealed decreased expressions of enzymes such as aspartate aminotransferase (GOT) and chorismate mutase (CM), which are involved in converting chorismate to tyrosine. Additionally, enzymes in the tyrosine catabolic pathway, including tyrosine aminotransferase (TAT) and pyruvate decarboxylase (PD), were downregulated in daughter corms. For instance, expression levels of *GOT1*, *CM*, *TAT*, and *PD* in the 0 N treatment were considerably higher (4.30, 2.89, 921.18, and 191.40 times, respectively) in mother corms compared to the 10 N treatment. Conversely, in daughter corms, the expression levels of *GOT1* and *CM* in the 0 N treatment were substantially lower (0.01 and 0.83, respectively) than in the 10 N treatment. Regarding isoquinoline alkaloid content in corms, the levels of hydromorphone and morphine were notably lower in the 0 N treatment compared to the 10 N treatment in both daughter and mother corms.

To verify the reliability of our RNA-seq results, we conducted a comparison between RNA-seq and qRT-PCR expression data for seven genes related to alkaloid biosynthesis (Fig. 9), correlation analysis confirmed the reproducibility of our RNA-seq results, with a correlation coefficient ($R^2 = 0.7511$, $p < 0.0001$).

Discussion

Differential responses of mother and daughter corms to nitrogen deficiency

As a storage organ, the corm provides energy and materials for leaf growth during periods when photosynthesis is insufficient [38, 39]. The consumption of mother corms reflects, to an extent, the energy they supply for the growth of other organs. Nitrogen deficiency can hinder energy conversion in mother corms, delaying the transition from mother to daughter corms. Our findings indicate that nitrogen deficiency significantly impacts the development of daughter corms, but has a minimal effect on mother corms. This suggests that daughter corm growth is more vulnerable to nitrogen shortages, making the period from the first to the second leaf maturity critical for nitrogen fertilization.

Under nitrogen-deficient conditions, the mother corm increases starch and sucrose metabolism while reducing the synthesis of various secondary metabolites. Nitrogen stress notably affects photosynthesis by decreasing the content and/or activity of light-harvesting proteins

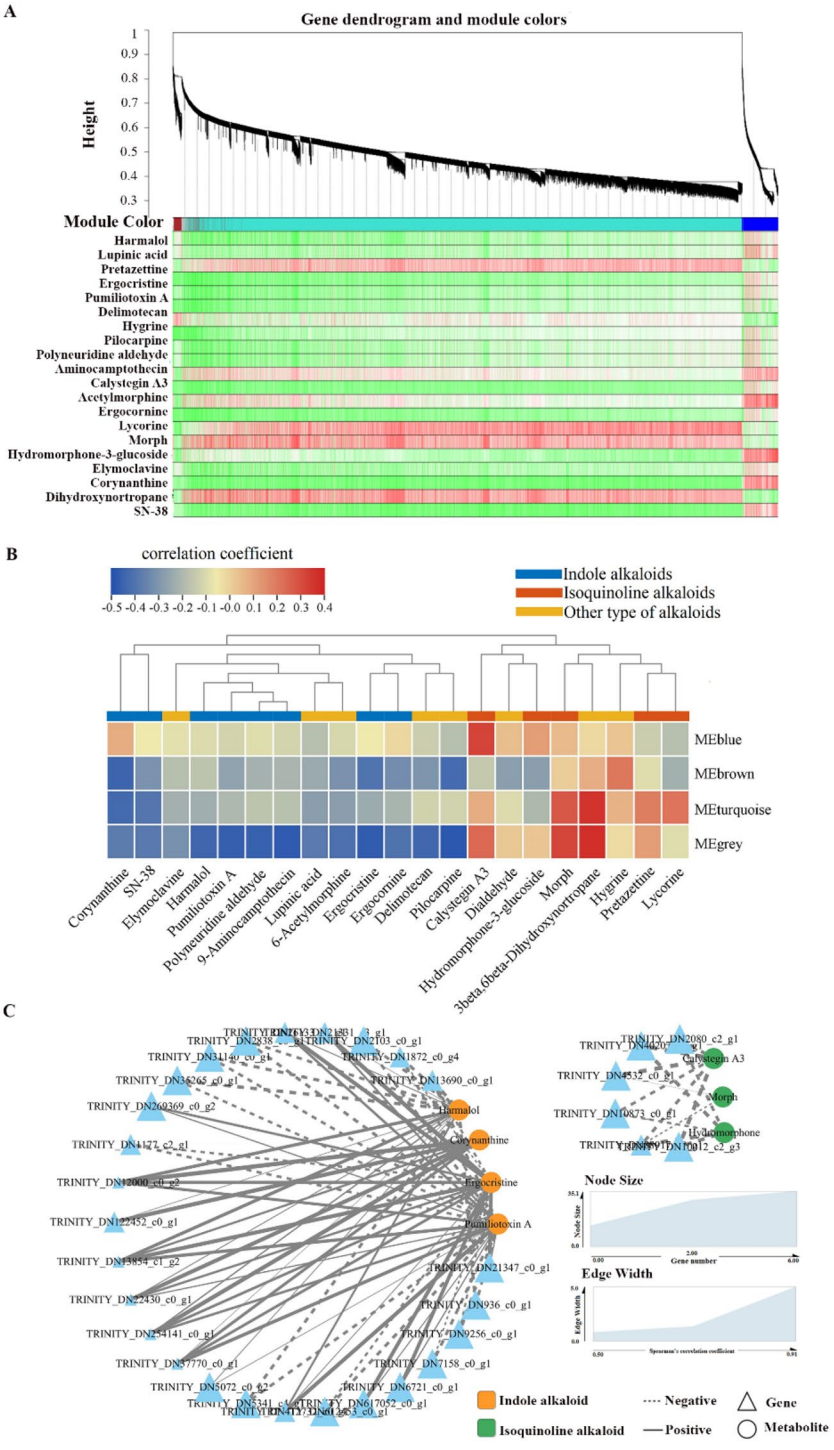

Fig. 7 Correlation analysis of genes related to alkaloid biosynthesis induced by nitrogen deficiency in corms of *A. muelleri*. Hierarchical cluster trees and coexpression modules identified by weighted gene coexpression network analysis in the corms (**A**). Different modules are labeled with different colors; the area in gray contains genes not belonging to any modules. The relevance of the modules to 21 alkaloids (**B**). Red indicates a positive correlation, and blue indicates a negative correlation. Visual display of module intergene correlations (**C**), in which each node represents a transcript. The greater the node connectivity (i.e., the greater the number of connections to other nodes, or the greater the number of radiating edges), the greater the importance

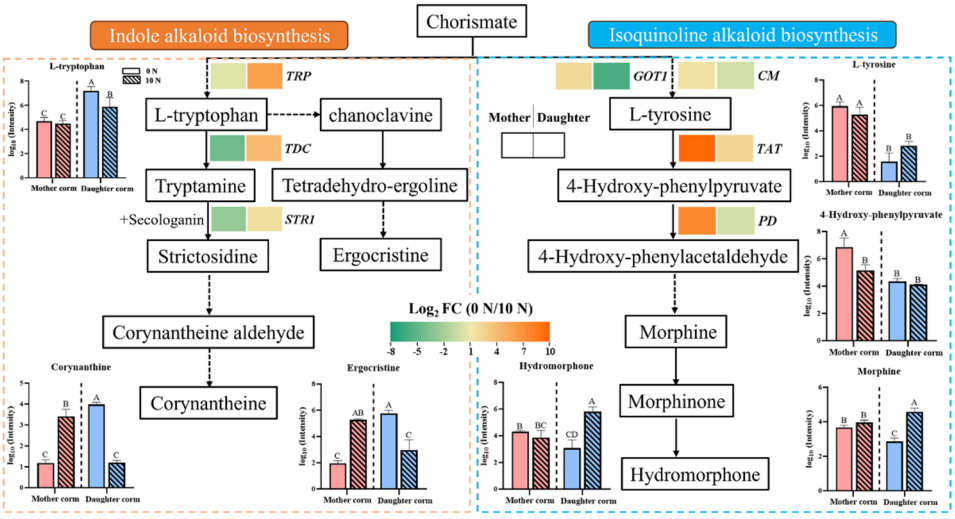

Fig. 8 Comparison of major alkaloids and genes involved in the indole and isoquinoline biosynthesis pathways between 0 N and 10 N treatments. Changes in transcript levels are indicated by color. At left is the mother corm, and at right is the daughter corm. Orange indicates upregulated gene expression, and green indicates downregulated expression. The values of the fold change (0 N vs. 10 N) are $\log_2$ scaled. The bar graphs represent the change in alkaloid content in the pathway, with red representing mother corms, blue representing daughter corms, solid colors representing the 0 N treatment, and diagonal stripes representing the 10 N treatment. The different letters above the bars indicate significant differences between developmental periods ($p < 0.05$; based on one-way ANOVA followed by a post hoc Tukey's test). Abbreviations: TRP: tryptophan synthase beta chain 2; TDC: tryptophan decarboxylase; STR: strictosidine synthase; GOT: aspartate aminotransferase; CM: chorismate mutase; TAT: tyrosine aminotransferase; PD: pyruvate decarboxylase

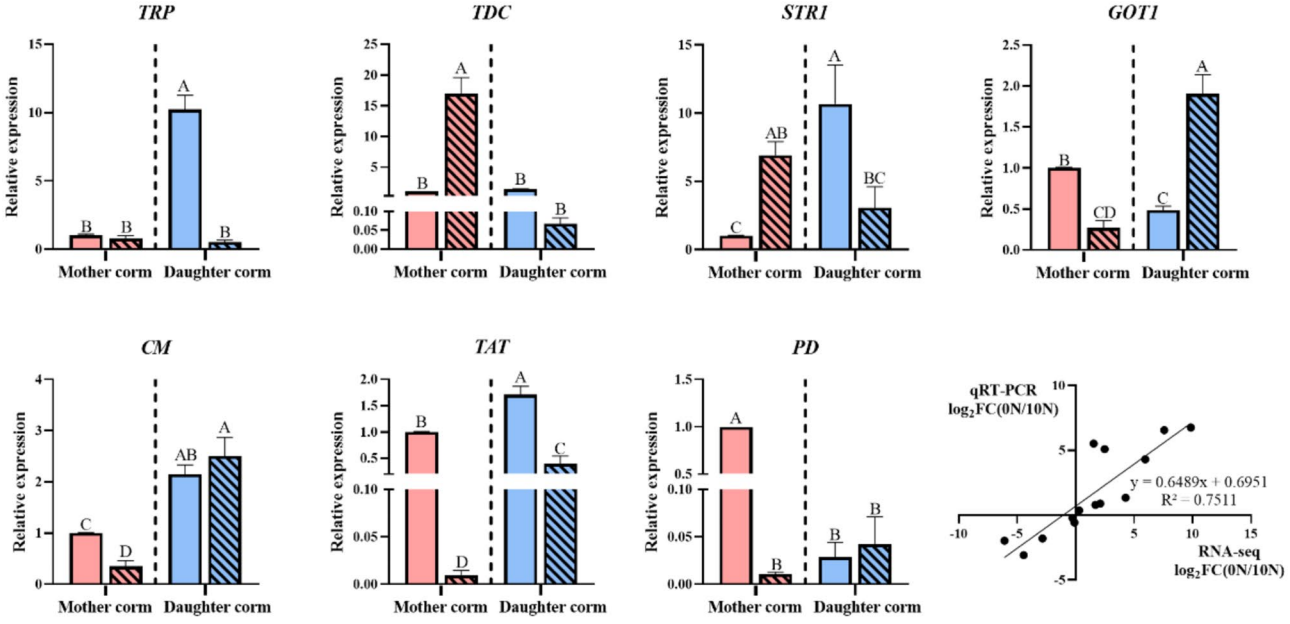

Fig. 9 Real-time quantitative PCR analysis of genes involved in the indole and isoquinoline biosynthesis pathways compared between corms of *A. muelleri* in the 0 N and 10 N treatments. The data indicate means ± standard deviations of three biological replicates. Red bars represent mother corms, blue bars represent daughter corms, solid colors represent the 0 N treatment, and diagonal stripes represent the 10 N treatment. The different letters above the bars indicate significant differences between developmental periods ($p < 0.05$; based on one-way ANOVA followed by a post hoc Tukey's test). The last graph is the Pearson correlation between RNA-seq and RT-qPCR

and photosynthetic enzymes [25]. Consequently, carbohydrate accumulation from photosynthesis is significantly limited [40, 41]. Enhanced metabolism of starch and sucrose in the mother corm may partially offset this lack of photosynthetic capability. The downregulation of secondary metabolite synthesis in the mother corm and delayed transformation are strategies that may be adopted to cope with nutrient deficiencies by moderating growth.

Conversely, starch and sucrose metabolism are reduced in daughter corms under nitrogen deficiency, while pathways such as phenylpropanoid and terpenoid backbone biosynthesis, along with induced systemic resistance, are enhanced. The suppression of sucrose and starch breakdown suggests that daughter corms may act as carbohydrate consumers rather than producers during their expansion growth phase. The biosynthesis of phenylpropanoids and terpenoid backbones, which are crucial for metabolite production in plants and play roles in abiotic stress response [42–45], indicates that daughter corms may bolster their defenses in response to nitrogen deficiency, balancing growth and defense needs.

The mother and daughter corms may have different alkaloid accumulation strategies

Nitrogen plays a critical role in the biosynthesis of alkaloids [10], which is a complex process influenced by multiple factors [46, 47]. In addition to nitrogen availability, precursor substances and developmental stages significantly impact alkaloid accumulation in konjac corms. Particularly, indole and isoquinoline alkaloids vary significantly during the developmental stages. The precursors for these alkaloids are aromatic amino acids—phenylalanine, tyrosine, and tryptophan [8, 10]—derived from the shikimate pathway. The availability of these amino acids is closely linked to alkaloid synthesis downstream [8, 48]. Our study revealed that L-tryptophan levels were notably higher in the early developmental stages of daughter corms compared to mother corms during the same period and increased further under nitrogen deficiency. Moreover, several genes promoting the synthesis and conversion of L-tryptophan to indole alkaloids [12, 49, 50] were significantly upregulated in daughter corms under nitrogen deprivation. This suggests that increased tryptophan levels in daughter corms provide a greater supply of precursors for indole alkaloid synthesis.

Tyrosine catabolism can be triggered by various factors such as wounding, fungal infections, or abiotic stresses like drought or nutritional deficiency [51–54]. This process leads to the production of isoquinoline alkaloids [12, 17]. Interestingly, while these alkaloids are resistant to stress, they do not tend to accumulate in daughter corms under nitrogen deficiency. Contrarily, in mother corms, isoquinoline alkaloids accumulate significantly under the same conditions, whereas daughter corms show an increase in indole alkaloids. This pattern suggests that under nitrogen deficiency, daughter corms preferentially convert chorismate into tryptophan to synthesize indole alkaloids, while mother corms convert it into tyrosine, boosting the production of isoquinoline alkaloids. Thus, mother and daughter corms may adopt different alkaloid accumulation strategies to cope with nitrogen deficiency as they develop.

Conclusion

This study enhances our understanding of alkaloid synthesis in konjac corms, highlighting the distinct patterns of alkaloid accumulation in corms of different ages under nitrogen-deficient conditions typical in konjac cultivation areas. It also supports the targeted extraction and utilization of konjac alkaloids. During alkaloid synthesis, enzymes such as TRP and GOT1 catalyze the formation of tryptophan and tyrosine, respectively, influencing the types of alkaloids accumulated. Additionally, our findings indicate that nitrogen deficiency significantly impacts the renewal process of corms, particularly inhibiting the growth and yield of daughter corms, marking this stage as crucial for nitrogen fertilizer application. This discovery offers a new perspective on the strategic use of nitrogen fertilizers in konjac cultivation.

Abbreviations

PCA	Principal component analysis
DEGs	Differentially expressed genes
KEGG	Kyoto encyclopedia of genes and genomes
kME	Module eigengene-based connectivity
TRP	Tryptophan synthase beta chain 2
TDC	Tryptophan decarboxylase
STR	Strictosidine synthase
GOT	Aspartate aminotransferase
CM	Chorismate mutase
TAT	Tyrosine aminotransferase
PD	Pyruvate decarboxylase

Supplementary Information

The online version contains supplementary material available at https://doi.org/10.1186/s12870-024-05642-z.

Supplementary Material 1: Table S1: The quality and concentration of the extracted RNA

Supplementary Material 2: Table S2: Sequences of primers used in RT-qPCR

Supplementary Material 3: Table S3: Effect of nitrogen deficiency on fresh weight and diameter of corms during the growth cycle of A. muelleri

Supplementary Material 4: Table S4: Analysis of nitrogen content in corms under different nitrogen levels

Supplementary Material 5: Table S5: Effect of nitrogen deficiency on metabolites in corms of A. muelleri

Supplementary Material 6: Table S6: Effect of nitrogen deficiency on the content of 21 alkaloids in corms of A. muelleri

Supplementary Material 7: Table S7: The expression of genes involved in the indole and isoquinoline biosynthesis pathways in corms of A. muelleri

Acknowledgements

I would like to thank Dr. Wei Zhang for his advice in the nitrogen treatment and Charlesworth group for providing language editing services.

Author contributions

Y.Q. performed the experiments, analyzed the data and drafted the manuscript. P.G., S.Y., and L.L. contributed to the data analysis, Y.K. and Y.Z. have revised and improved the manuscript. L.Y. and F.H. conducted the conceptualization, methodology, and supervision. All authors contributed to the article and approved the submitted version.

Funding
This study was supported by Yunnan Fundamental Research Projects (NO. 202101BA070001-163), Yunnan Province Youth Talent Support Program (No. 202101AU070047), Yunnan Provincial Science and Technology Department (No. 202301AT070055). Kunming University Talent Support Program (No. XJ20230017).

Data availability
The RNA-seq data used in the study have been deposited in the Gene Expression Omnibus under code PRJNA1023371.

Declarations

Ethics approval and consent to participate
Not applicable.

Consent for publication
Not applicable.

Competing interests
The authors declare no competing interests.

Author details
[1]College of Agronomy, Yunnan Key Laboratory of Konjac Biology, Yunnan Urban Agricultural Engineering and Technological Research Center, Kunming University, Kunming 650214, China

Received: 25 July 2024 / Accepted: 26 September 2024
Published online: 03 October 2024

References

1. Claudel C, Buerki S, Chatrou LW, Antonelli A, Alvarez N, Hetterscheid W. Large scale phylogenetic analysis of *Amorphophallus* (Araceae) derived from nuclear and plastid sequences reveals new subgeneric delineation. Bot J Linn Soc. 2017;184:32–45.
2. Zhang SL, Liu PY, Zhang XG, Zhang YJ, Su CG. China resources of Konjac development and utilization program in China. J Southwest Agri Univ. 1999;270:593–601.
3. Liu P. In: Konjac, editor. Chemical composition of Konjac. Beijing: China Agriculture; 2004. pp. 214–5.
4. Mutaqin AZ, Kurniadie D, Iskandar J, Nurzaman M, Husodo T. Morphological characteristics and habitat conditions of suweg (*Amorphophallus paeoniifolius*) around Mount Ciremai National Park, West Java, Indonesia. Biodiversitas J Biol Divers. 2021;22:2591–600.
5. Adamski Z, Blythe LL, Milella L, Bufo SA. Biological activities of alkaloids: from toxicology to pharmacology. Toxins. 2020;12:210.
6. Zhang DH, Wang Q. Biology characteristic and prospect of *Amorphophallus muelleri* in plantation of Konjac. J C Veg. 2010;22:71–3.
7. Pillay R, Chemban FM, Pillay VV, Rathish B. Little known dangers of an exotic poisonous fruit: lessons from two cases of konjac ingestion. Cureus. 2020;12:e11972.
8. Aniszewski T. Alkaloid chemistry. Alkaloids: Chemistry, Biology, Ecology, and applications, edition 2. Amsterdam: Elsevier; 2015. pp. 99–193.
9. Matsuura H, Fett-Neto AG. Plant alkaloids: main features, toxicity, and mechanisms of action. Plant Toxins. 2015;2:1–15.
10. Gutiérrez-Grijalva EP, López-Martínez LX, Contreras-Angulo LA, Elizalde-Romero CA, Heredia JB. Plant alkaloids: structures and bioactive properties. In Plant-derived Bioactives: Chemistry and Mode of Action, edition 1., Swamy, M. K., Eds., Springer: Singapore, 2020;85–117.
11. Guirimand G, Courdavault V, St-Pierre B, Burlat V. Biosynthesis and regulation of alkaloids. In: Davey EC, M. R., editor. Plant Developmental Biology - Biotechnological Perspectives, edition 1, Pua. Berlin: Springer-; 2010. pp. 139–60.
12. Facchini PJ, Huber-Allanach KL, Tari LW. Plant aromatic L-amino acid decarboxylases: evolution, biochemistry, regulation, and metabolic engineering applications. Phytochem. 2000;54(2):121–38.
13. Valipour M, Hosseini A, Di Sotto A, Irannejad H. Dual action anti-inflammatory/antiviral isoquinoline alkaloids as potent naturally occurring anti-SARS-CoV-2 agents: a combined pharmacological and medicinal chemistry perspective. Phytother Res. 2023;37(5):2168–86.
14. Yun D, Yoon SY, Park SJ, Park YJ. The anticancer effect of natural plant alkaloid isoquinolines. Int J Mol Sci. 2021;22(4):1653.
15. Girard-Valenciennes SSAL, Septembre-Malaterre E, Gasque A, Guiraud P, Sélambarom P. Anti-alphaviral alkaloids: focus on some isoquinolines, indoles and quinolizidines. Mol. 2022;27(16):5080.
16. De Luca V, St Pierre B. The cell and developmental biology of alkaloid biosynthesis. Trends Plant Sci. 2000;5:168–73.
17. Facchini PJ, Bird DA, St-Pierre B. Can *Arabidopsis* make complex alkaloids? Trends Plant Sci. 2004;9(3):116–22.
18. Lichman B. The scaffold-forming steps of plant alkaloid biosynthesis. Nat Prod Rep. 2020;38:103–29.
19. Gojon A. Nitrogen nutrition in plants: rapid progress and new challenges. J Exp Bot. 2017;68(10):2457–62.
20. Zheng Y, Zhang X, Liu X, Qin N, Xu K, Zeng R, Liu J, Song Y. Nitrogen supply alters rice defense against the striped stem borer *Chilo Suppressalis*. Front Plant Sci. 2021;12:691292.
21. Barłóg P. Effect of magnesium and nitrogenous fertilisers on the growth and alkaloid content in *Lupinus angustifolius* L. Crop Pasture Sci. 2002;53(6):671–6.
22. Zhang L, Chen Z, Ma X, Zhao Y. Effect of different nitrogen concentrations on the growth and contents of berberine in rhizome of *Coptis Chinensis* Franch. Chin J Chin Mat Med. 1998;23:394–6.
23. Shi SL, Tang XQ, Nie PQ, Ye BZ, Zhang RZ, Wang KC. Effects of nitrogen deficiency and nitrogen restitution on nutrition and active components of *Isatis Indigotica* at seedling stage. Nanjing Agric Univ. 2015;38(5):780–6.
24. Chen G, Zhang Z, Guo Q, Wang X, Wen Q. Quantitative assessment of soil erosion based on CSLE and the 2010 national soil erosion survey at regional scale in Yunnan Province of China. Sustainability. 2019;11:3252.
25. Mu X, Chen Y. The physiological response of photosynthesis to nitrogen deficiency. Plant Physiol Biochem. 2021;158:76–82.
26. Huot B, Yao J, Montgomery BL, He SY. Growth-defense tradeoffs in plants: a balancing act to optimize fitness. Mol Plant. 2014;7:1267–87.
27. He Z, Webster S, He SY. Growth-defense trade-offs in plants. Curr Biol. 2022;32(12):634–9.
28. Campbell MA, Gleichsner A, Alsbury R, Horvath D, Suttle J. The sprout inhibitors chlorpropham and 1,4-dimethylnaphthalene elicit different transcriptional profiles and do not suppress growth through a prolongation of the dormant state. Plant Mol Biol. 2010;73:181–9.
29. Wen B, Mei Z, Zeng C, Liu S. metaX: a flexible and comprehensive software for processing metabolomics data. BMC Bioinf. 2017;18:183.
30. Grabherr MG, Haas BJ, Yassour M, Levin JZ, Thompson DA, Amit I, Adiconis X, Fan L, Raychowdhury R, Zeng Q, Chen Z, Mauceli E, Hacohen N, Gnirke A, Rhind N, di Palma F, Birren BW, Nusbaum C, Lindblad-Toh K, Friedman N, Regev A. Full-length transcriptome assembly from RNA-Seq data without a reference genome. Nat Biotechnol. 2011;29(7):644–52.
31. Li B, Dewey CN. RSEM: accurate transcript quantification from RNA-seq data with or without a reference genome. BMC Bioinf. 2011;12:323.
32. Love MI, Huber W, Anders S. Moderated estimation of Fold change and dispersion for RNA-seq data with DESeq2. Genome biol. 2014;15(12):550.
33. Xie C, Mao X, Huang J, Ding Y, Wu J, Dong S, Kong L, Gao G, Li CY, Wei L. KOBAS 2.0: a web server for annotation and identification of enriched pathways and diseases. Nucleic Acids Res. 2011;39:316–22.
34. Langfelder P, Horvath S. WGCNA: an R package for weighted correlation network analysis. BMC Bioinformatics. 2008;9:559.
35. Shannon P, Markiel A, Ozier O, Baliga NS, Wang JT, Ramage D, Amin N, Schwikowski B, Ideker T. Cytoscape: a software environment for integrated models of biomolecular interaction networks. Genome Res. 2003;13(11):2498–504.
36. Mestdagh P, Van Vlierberghe P, De Weer A, Muth D, Westermann F, Speleman F, Vandesompele J. A novel and universal method for microRNA RT-qPCR data normalization. Genome Biol. 2009;10(6):64.
37. Chen C, Chen H, Zhang Y, Thomas HR, Frank MH, He Y, Xia R. TBtools: an integrative toolkit developed for interactive analyses of big biological data. Mol Plant. 2020;13:1194–202.
38. Villordon AQ, Ginzberg I, Firon N. Root architecture and root and tuber crop productivity. Trends Plant Sci. 2014;19:419–25.
39. Akoumianakis KA, Alexopoulos A, Karapanos I, Kalatzopoulos K, Aivalakis G, Passam H. Carbohydrate metabolism and tissue differentiation during potato tuber initiation, growth and dormancy induction. Aust J Crop Sci. 2016;10:185–92.
40. Hofius D, Börnke FAJ. Photosynthesis, carbohydrate metabolism and source–sink relations. In: Bradshaw D, Gebhardt J, C., et al. editors. Potato Biology

and Biotechnology, edition 1., Vreugdenhil. Amsterdam: Elsevier; 2007. pp. 257–85.
41. Treves H, Küken A, Arrivault S, Ishihara H, Hoppe I, Erban A, Höhne M, Moraes TA, Kopka J, Szymanski J, Nikoloski Z, Stitt M. Carbon flux through photosynthesis and central carbon metabolism show distinct patterns between algae, C_3 and C_4 plants. Nat Plants. 2022;8:78–91.
42. Fraser CM, Chapple C. The phenylpropanoid pathway in *Arabidopsis*. Arabidopsis Book. 2011;9:e0152.
43. Kazan K. Diverse roles of jasmonates and ethylene in abiotic stress tolerance. Trends Plant Sci. 2015;20:219–29.
44. Yang C, Li W, Cao J, Meng F, Yu Y, Huang J, Jiang L, Liu M, Zhang Z, Chen X, Miyamoto K, Yamane H, Zhang J, Chen S, Liu J. Activation of ethylene signaling pathways enhances disease resistance by regulating ROS and phytoalexin production in rice. Plant J. 2017;89:338–53.
45. Sharma A, Shahzad B, Rehman A, Bhardwaj R, Landi M, Zheng B. Response of phenylpropanoid pathway and the role of polyphenols in plants under abiotic stress. Molecules. 2019;24(13):2452.
46. Otterbach SL, Yang T, Kato L, Janfelt C, Geu-Flores F. Quinolizidine alkaloids are transported to seeds of bitter narrow-leafed lupin. J Exp Bot. 2019;70(20):5799–808.
47. Divekar PA, Narayana S, Divekar BA, Kumar R, Gadratagi BG, Ray A, Singh AK, Rani V, Singh V, Singh AK, Kumar A, Singh RP, Meena RS, Behera TK. Plant secondary metabolites as defense tools against herbivores for sustainable crop protection. Int J Mol Sci. 2022;23(5):2690.
48. Richter U, Rothe G, Fabian AK, Rahfeld B, Dräger B. Overexpression of tropinone reductases alters alkaloid composition in *Atropa belladonna* root cultures. J Exp Bot. 2005;56(412):645–52.
49. Runguphan W, Maresh JJ, O'Connor SE. Silencing of tryptamine biosynthesis for production of nonnatural alkaloids in plant culture. Proc Natl Acad Sci. 2009;106(33):13673–8.
50. Ramani S, Patil N, Nimbalkar S, Jayabaskaran C. Alkaloids derived from tryptophan: rerpenoid indole alkaloids. Natural products: Phytochemistry, Botany and Metabolism of alkaloids, phenolics and terpenes. Edition 1, Ramawat KG, Mérillon JM. Berlin: Eds., Springer; 2013. pp. 575–604.
51. Guillet G, De Luca V. Wound-inducible biosynthesis of phytoalexin hydroxycinnamic acid amides of tyramine in tryptophan and tyrosine decarboxylase transgenic tobacco lines. Plant Physiol. 2005;137(2):692–9.
52. Liu X, Jin Y, Tan K, Zheng J, Gao T, Zhang Z, Zhao Y, Ma F, Li C. *MdTyDc* overexpression improves alkalinity tolerance in *Malus domestica*. Front Plant Sci. 2021;12:625890.
53. Wang Y, Chen Q, Zheng J, Zhang Z, Gao T, Li C, Ma F. Overexpression of the tyrosine decarboxylase gene *MdTyDC* in apple enhances long-term moderate drought tolerance and WUE. Plant Sci. 2021;313:111064.
54. Liu Y, Liu Q, Li X, Tang Z, Zhang Z, Gao H, Ma F, Li C. Exogenous dopamine and *MdTyDC* overexpression enhance apple resistance to *Fusarium solani*. Phytopathol. 2022;112(12):2503–13.

Publisher's note